6ICEGE 6th International Conference on Earthquake Geotechnical Engineering
1-4 November 2015
Christchurch, New Zealand

Assessment of the Relative Predictive Capabilities of CPT-Based Liquefaction Evaluation Procedures: Lessons Learned from the 2010-2011 Canterbury Earthquake Sequence

R.A. Green[1], B.W. Maurer[2], M. Cubrinovski[3], B.A. Bradley[4]

ABSTRACT

Data from the 2010-2011 Canterbury earthquake sequence (CES) provides an unprecedented opportunity to assess and advance the current state of practice for evaluating liquefaction triggering. Towards this end, select case histories from the CES are used herein to assess the predictive capabilities of three alternative CPT-based simplified liquefaction evaluation procedures: Robertson and Wride (1998); Moss et al. (2006); and Idriss and Boulanger (2008). Additionally, the Liquefaction Potential Index (LPI) framework for predicting the severity of surficial liquefaction manifestations is also used to assess the predictive capabilities of the liquefaction evaluation procedures. Although it is not without limitations, use of the LPI framework for this purpose circumvents the need for selecting "critical" layers and their representative properties for study sites, which inherently involves subjectivity and thus has been a point of contention among researchers. It was found that while all the assessed liquefaction triggering evaluation procedures performed well for the parameter ranges of the sites analyzed, the procedure proposed by Idriss and Boulanger (2008) yielded predictions that are more consistent with field observations than the other procedures. However, use of the Idriss and Boulanger (2008) procedure in conjunction with a Christchurch-specific correlation to estimate fines content showed a decreased performance relative to using a generic fines content correlation. As a result, the fines correction for the Idriss and Boulanger (2008) procedure needs further study.

Introduction

The 2010-2011 Canterbury earthquake sequence (CES) began with the 4 September 2010, M_w7.1 Darfield earthquake and included up to ten events that induced liquefaction (Quigley et al., 2013). Widespread liquefaction was, however, most notably induced by the M_w7.1, 4 September 2010 Darfield and the M_w6.2, 22 February 2011 Christchurch earthquakes. The ground motions from these events were recorded across Christchurch and its environs by a dense network of strong motion stations (e.g., Cousins and McVerry, 2010; Bradley and Cubrinovski, 2011; Bradley, 2012a). Also, due to the severity and spatial extent of liquefaction resulting from the 2010-2011 earthquakes and its impacts on residential land, the New Zealand Earthquake

[1]Professor, Department of Civil and Environmental Engineering, Virginia Tech, Blacksburg, Virginia, USA, rugreen@vt.edu
[2]Doctoral Student, Department of Civil and Environmental Engineering, Virginia Tech, Blacksburg, Virginia, USA, bwmaurer@vt.edu
[3]Professor, Department of Civil and Natural Resources Engineering, University of Canterbury, Christchurch, New Zealand, misko.cubrinovski@canterbury.ac.nz
[4]Associate Professor, Department of Civil and Natural Resources Engineering, University of Canterbury, Christchurch, New Zealand, brendon.bradley@canterbury.ac.nz

Commission (EQC) funded an extensive subsurface characterization program for Christchurch, with over 20,000 Cone Penetration Test (CPT) soundings performed to date.

The combination of well-documented liquefaction response during multiple events, densely-recorded ground motions for the events, and detailed subsurface characterization provides an unprecedented opportunity to assess and advance the current state of practice for evaluating liquefaction triggering. Towards this end, the authors herein update a previous study they performed (Green et al., 2014) that used select case histories to evaluate commonly used deterministic, CPT-based simplified liquefaction evaluation procedures, namely the procedures proposed by Robertson and Wride (1998) (RW98), Moss et al. (2006) (Mea06), and Idriss and Boulanger (2008) (IB08). These procedures were assessed by comparing predicted to observed liquefaction responses at the case history sites. The update of this comparison includes the removal of one CPT sounding from the study due to questions about the accuracy of the recorded sleeve friction and use of a revised Christchurch-specific correlation for estimating fines content (FC). An error index proposed by Green et al. (2014) is used to quantify the predictive capabilities of the three CPT-based procedures for the selected case histories.

While simplified liquefaction evaluation procedures provide estimates of the factor of safety (FS) against liquefaction triggering as a function of depth in a profile, they do not predict the severity of liquefaction manifestation at the ground surface, which more directly correlates to damage potential due to liquefaction. To fill this gap, Iwasaki et al. (1978) proposed the liquefaction potential index (LPI) to better characterize the damage potential of liquefaction. The LPI framework assumes that the severity of liquefaction manifestation is proportional to the thickness of a liquefied layer; the amount by which FS is less than 1.0; and the proximity of the layer to the ground surface. For example, within the LPI framework a thick, shallow layer with a low computed FS would be predicted to result in more severe surficial liquefaction manifestations than would a thinner, deeper layer that has the same computed FS.

The LPI framework is used herein to assess the consistency of the predictions of the alternative CPT-based simplified liquefaction evaluation procedures to field observations. In contrast to using a limited number of select case histories for this purpose, as mentioned above, no additional judgement is needed within the LPI framework to select “critical layers” and their representative properties, which is often a point of contention among researchers. Rather, the liquefaction response of the entire profile is considered in the LPI framework. Also, circumventing the need to select critical layers and their representative properties allows a larger number (i.e., thousands) of CPT soundings to be used in the evaluation process. However, use of the LPI has drawbacks and should be viewed as an alternative approach to assessing the predictive capabilities of the liquefaction evaluation procedures, rather than a superior approach. Specifically, issues with the depth weighting factor (e.g., van Ballegooy et al., 2014a; Maurer et al., 2015c) and the lack of accounting for the influence of the non-liquefiable crust and interbedded non-liquefiable layers on the severity of surficial manifestations (Maurer et al. 2015a,c) are inherent limitations of the LPI procedure.

In the remaining sections of this paper, background information on geology of the Canterbury

Plains and on the Darfield and Christchurch earthquakes is presented first, with emphasis on information relevant to liquefaction. Next, the ground motions recorded during the Darfield and Christchurch earthquakes are discussed in relation to how the peak ground accelerations (PGA) at study sites were estimated. This is followed by an updated assessment of CPT-based liquefaction evaluation procedures using select case histories from the Canterbury region. Finally, the same liquefaction evaluation procedures are then assessed using the LPI framework.

Geology and Geomorphology of the Christchurch Area

The Canterbury Plains are ~160 km long and up to 60 km wide. The plains are the result of overlapping alluvial fans produced by glacier-fed rivers from the Southern Alps, the main mountain range of the South Island (Forsyth et al., 2008). Uplift of the Southern Alps resulted in rapid deposition during the late Quaternary and inundation of the Canterbury Plains by alluvial and fluvial sediments. The alluvial gravels underlying the Canterbury Plains typically have thicknesses of at least 500 m. Most of the soils in the region are derived from greywacke from the Southern Alps or from loess (fine silt blown from riverbeds). In addition, some deposits in southern Christchurch include clay and other minerals eroded from the extinct volcanic complex forming Banks Peninsula (Brown et al., 1995).

Most of Christchurch was once low-lying floodplains and swamps behind a series of barrier dunes (composed of fine-grained beach/dune sand), estuaries, and lagoons (underlain by fine-grained deposits) of Pegasus Bay. The Waimakariri River regularly flooded Christchurch before stopbank construction and river realignment, shortly after the city was established in 1850. The original city center was constructed on slightly higher ground compared to areas to the north and east. Of particular relevance to liquefaction susceptibility in Christchurch and its environs are the locations of abandoned paleo-channels of the Waimakariri, Heathcote, and Avon Rivers, and former swamps. These areas are underlain by, and filled with, young loose sandy sediments, with shallow groundwater levels (from 1 to 5 m below ground surface), which are highly susceptible to liquefaction (e.g., Wotherspoon et al., 2012).

Samples of liquefaction ejecta were collected from several sites around Christchurch and Kaiapoi. The grain characteristics of these samples were analyzed using a scanning electron microscope (SEM), energy-dispersive x-ray spectrometry (EDS), x-ray diffraction (XRD), and a laser particle size analyzer. Although the characteristics of the collected samples varied, most can be described as silty fine sand having subrounded particle shapes. The EDS and XRD analyses showed that the ejecta is predominantly quartz and feldspar, which is consistent with the hypothesis that the material was derived from Torlesse Greywacke sandstone in the Southern Alps. The grain size distributions obtained from the laser particle size analyses indicate that the samples classify as SP, SM, and SP-SM per ASTM D-2487 (ASTM, 2011).

Ground Motions

Both the M_w7.1, 4 September 2010 Darfield earthquake and the M_w6.2, 22 February 2011 Christchurch earthquake were damaging and caused widespread liquefaction (e.g., Cubrinovski

et al., 2011; Green et al., 2011a,b; Orense et al., 2011; Cubrinovski et al., 2012; Robinson et al., 2013; Maurer et al., 2014a). However, due to the close proximity of its rupture plane, the Christchurch earthquake resulted in more intense shaking in much of Christchurch and resulted in 185 fatalities, while the epicenter of the Darfield earthquake was in a more rural area and did not result in any fatalities.

The motions from both the Darfield and Christchurch earthquakes were recorded by a dense network of strong ground motion stations (e.g., Cousins and McVerry, 2010; Bradley and Cubrinovski, 2011; Bradley, 2012b; Bradley, 2012c; Bradley et al., 2014). To evaluate the factor of safety against liquefaction per the simplified procedures used herein, the amplitude of cyclic loading is assumed to be proportional to the PGA at the ground surface and the duration is assumed to be related to the earthquake magnitude. Using the accelerograms recorded at the strong motion stations (GeoNet, 2012), the conditional PGA distributions at the case history sites were computed using the procedure detailed in Bradley (2014a), which have been previously utilized by Green et al. (2011, 2014) and Maurer et al. (2014a,b, 2015a,b). Contour maps of the computed median conditional PGAs for the Darfield and Christchurch earthquakes are shown in Figure 1.

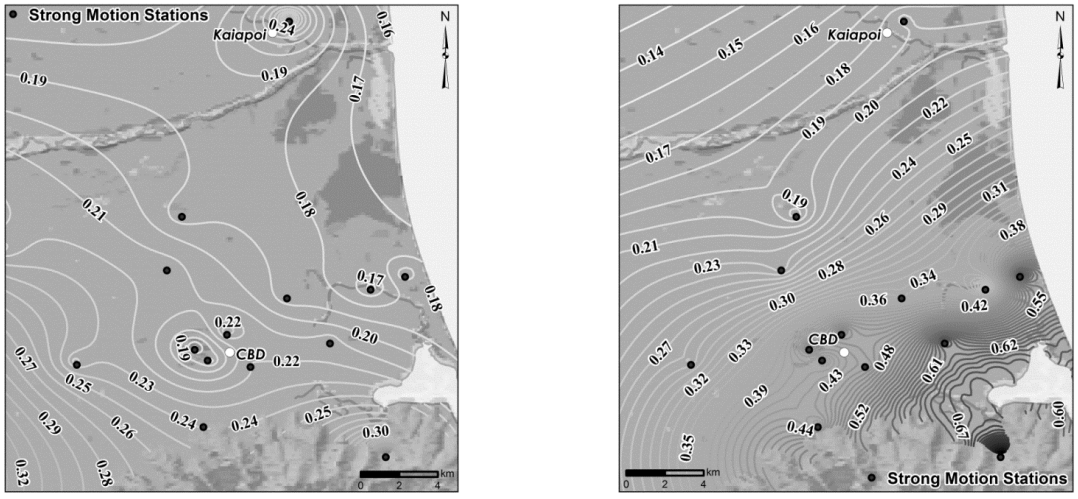

(a) (b)

Figure 1. Contours of computed median conditional PGAs (g): (a) Darfield earthquake; and (b) Christchurch earthquake.

Evaluation of CPT Liquefaction Evaluation Procedures Using Select Liquefaction Case Histories

Case History Sites

As mentioned above, and as shown in Figure 2, widespread liquefaction was induced during both the Darfield and Christchurch earthquakes. While there was certainly significant overlap in the areas that liquefied during these events, there were also areas that liquefied during the Darfield

event that had no or only minor surficial liquefaction manifestations resulting from the Christchurch event, or vice versa. It was these areas that Green et al. (2014) targeted for further investigation because these sites would seemingly yield data that would best constrain the position of a Cyclic Resistance Ratio (CRR) curve. Additionally, in order to minimize the uncertainty in the seismic loading at the sites, Green et al. (2014) further refined the targeted sites to those that were relatively close to strong motion stations.

Green et al. (2014) provide detailed information on 25 selected sites. The locations of these sites, which are presented in Figure 2 and Table 1, are primarily located in three general areas: (1) Christchurch's Central Business District (CBD), (2) north eastern suburbs of Christchurch, and (3) north and south Kaiapoi. Re-evaluation of the CPT sounding data for these sites has resulted in the exclusion of one of them from this study (i.e., Site 2: AVD-07) due to issues with the recorded sleeve friction (van Ballegooy, 2015). Each of the remaining 24 selected sites are analyzed herein using the RW98, Mea06, and IB08 CPT-based, deterministic simplified liquefaction evaluation procedures for the Darfield and Christchurch earthquakes, resulting in 48 case histories. For the IB08, the FC for the critical layers for the selected sites are estimated using two different correlations, one that was previously used by Green et al. (2014) and the other that is proposed herein.

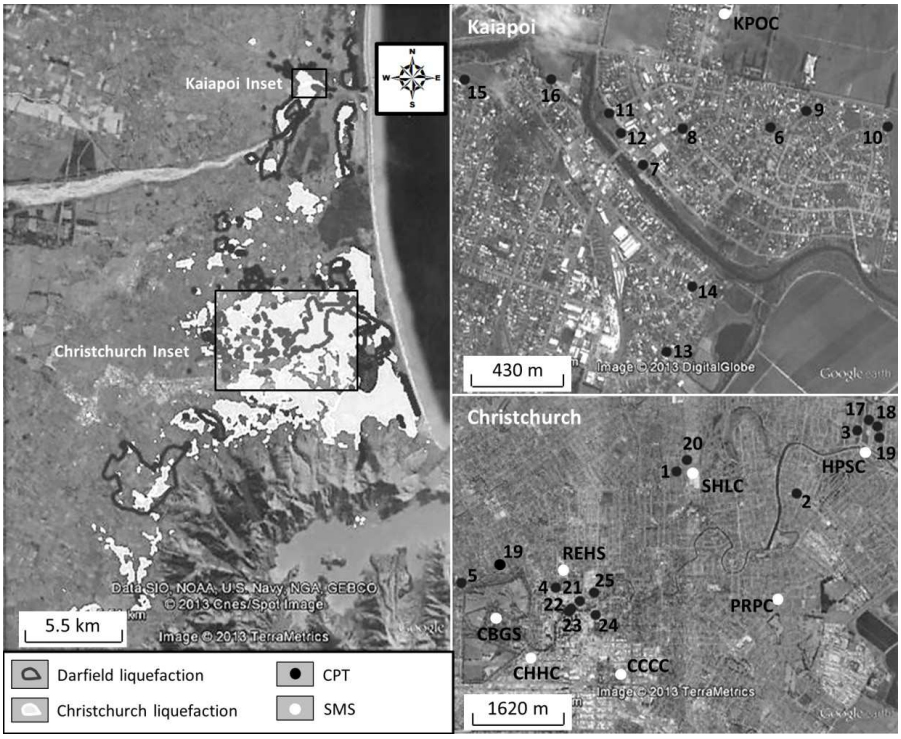

Figure 2. Left: Areas that liquefied during the M_w7.1 Darfield earthquake (bound by dark lines) and areas that liquefied during the M_w6.2 Christchurch earthquake (white shaded areas). Right: Locations of case history sites (numbered, dark dots) and strong motion seismograph stations (labeled, white dots).

Table 1. General site/profile data for case history sites.

No.	Site Name[1]	Latitude (degrees)	Longitude (degrees)	Liq Response (Darfield Eqk)	Liq Response (Chch Eqk)	Critical Depth Range (m)
1	SHY-09	-43.50520	172.66001	No Liq	Mod Liq	3.80-5.75
~~2~~	~~AVD-07~~	~~-43.50848~~	~~172.68695~~	~~No Liq~~	~~Mod Liq~~	~~2.50-4.50~~
3	BUR-46	-43.49811	172.70027	Minor Liq	Severe Liq	5.75-8.75
4	CBD-21	-43.52436	172.63342	No Liq	Minor Liq	4.50-6.50
5	FND-01	-43.52377	172.61232	Mod Liq/Lat Sprd	Sev Lat Sprd	3.60-3.90
6	KAN-03	-43.38126	172.66664	Minor Liq	No Liq	3.75-6.70
7	KAN-05	-43.38295	172.65910	Minor Liq	Minor Liq	3.15-4.10
8	KAN-09	-43.38137	172.66143	Minor Liq	No Liq	1.25-2.45
9	KAN-19	-43.38053	172.66875	Minor Liq	No Liq	2.35-5.00
10	KAN-23	-43.38115	172.67360	Minor Liq	No Liq	4.30-5.30
11d	KAN-26d	-43.38075	172.65704	Mod Liq	NA	4.90-8.00
11c	KAN-26c	-43.38075	172.65704	NA	Minor Liq	1.50-2.40
12	KAN-28	-43.38160	172.65777	Minor-Mod Liq	Minor Liq	2.00-3.15
13	KAS-08	-43.39104	172.66066	Minor-Mod Liq	Minor Liq	1.30-2.65
14	KAS-11	-43.38819	172.66213	Minor-Mod Liq	Minor Liq	2.00-3.10
15	KAS-20	-43.37939	172.64842	Minor-Mod Liq	Minor Liq	3.50-5.00
16	KAS-40	-43.37932	172.65357	Minor-Mod Liq	Minor Liq	1.90-2.75
17	SNB-01	-43.49636	172.70281	Minor Liq	Severe Liq	2.25-5.00
18	NBT-02	-43.49739	172.70474	Minor-Mod Liq	Severe Liq	4.80-6.70
19	NBT-03	-43.49919	172.70525	Minor Liq	Severe Liq	7.00-10.20
20	RCH-14	-43.50330	172.66232	No Liq	Minor-Mod Liq	3.50-5.50
21	Z1-3	-43.52648	172.63882	Minor Liq	Mod-Sev Liq	4.00-8.25
22	Z2-11	-43.52822	172.63646	No Liq	Mod Liq	2.20-3.30
23	Z2-6	-43.52772	172.63697	No Liq	Lat Sprd	2.00-2.85
24	Z4-4	-43.52867	172.64241	No Liq	Mod Liq	2.00-3.25
25	Z8-11	-43.52506	172.64200	Minor-Mod Liq	Mod-Sev Liq	1.40-2.25

[1]KAN-26d and KAN-26c list the data for KAN-26 for the Darfield (d) and Christchurch (c) earthquakes, respectively.

Evaluation of Existing Liquefaction Evaluation Procedures

In Figure 3, the case history data are plotted together with the CRR curves for each of the three liquefaction evaluation procedures. The plotted CRR curves are for M_w7.5 (i.e., $CRR_{M7.5}$), "clean sand," 1 atm initial vertical effective confining stress (σ'_{v0}), and level ground conditions. For the Mea06 procedure, the "nonlinear shear mass participation factor" (r_d) can be computed two ways, depending on whether the average shear wave velocity in the upper 12 m of the profile (V_{S12}) for the site is known or not. Since surface wave testing was performed at each site, the authors computed the $CSR_{M7.5}$ (i.e., cyclic stress ratios normalized to a M_w7.5 earthquake) for the sites using both V_{S12}-independent and -dependent r_d equations, where the former equation is given in Moss et al. (2006) and the latter in Cetin (2000). Both sets of $CSR_{M7.5}$ data are shown in Figure 3b, where the triangular and circular symbols correspond to the values computed using the V_{S12}-dependent r_d equations and the "end of the tails" extending from the triangular and circular symbols correspond to the values computed using the V_{S12}-independent r_d equations. As may be observed from this figure, the predictive capabilities of the Mea06 procedure improves when $CSR_{M7.5}$ is computed using the V_{S12}-dependent r_d equation proposed by Cetin (2000).

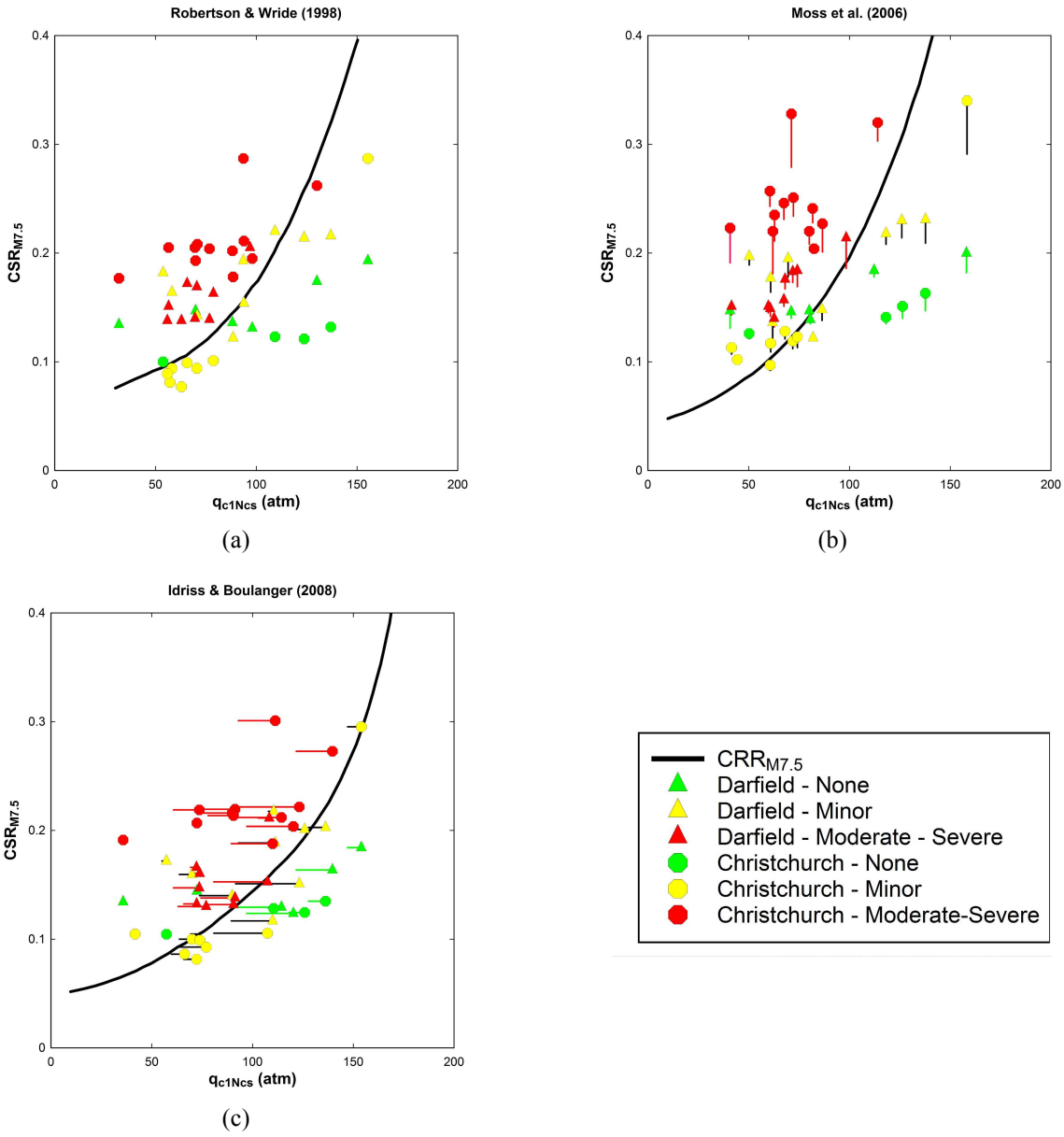

Figure 3. Case history data plotted together with $CRR_{M7.5}$ curves:
(a) RW98; (b) Mea06; (c) IB08.

Fines content is required to compute normalized tip resistance per IB08, while normalized tip resistances per the RW98 and Mea06 are based on I_c and R_f, respectively. The FC of the critical layers were estimated using two different I_c-FC correlations, a generic correlation proposed by Robertson and Wride (1998) and a new Christchurch-specific correlation proposed herein (Figure 4); note that the latter relation differs from the early Christchurch-specific I_c-FC correlation used by Green et al. (2014), which was developed by Robinson et al. (2013). Also, it should be noted that Idriss and Boulanger (2008) do not recommend the use of generic I_c-FC correlations to estimate FC, but rather recommend the development and use of project-specific

I_c-FC correlations such as that shown in Figure 4. The Christchurch-specific correlation shown in Figure 4 was developed from a statistical regression of data from 2,400 soil samples obtained from 700 sites throughout Christchurch. For comparison purposes, the Robertson and Wride (1998) generic I_c-FC correlation, which is also used in this study, is also plotted in Figure 4.

The authors computed normalized CPT tip resistances per IB08 for the case histories using the FC estimated using both I_c-FC correlations. The $CSR_{M7.5}$ case history data for IB08 are plotted in Figure 3c. In this figure, the triangular and circular symbols correspond to the normalized CPT tip resistances computed using FC values estimated using the new Christchurch-specific I_c-FC correlation. The "end of the tails" extending from the triangular and circular symbols correspond to the normalized CPT tip resistances computed using FC values estimated using the Robertson and Wride (1998) generic I_c-FC correlation. For most of the cases analyzed herein, the new Christchurch-specific correlation resulted in a larger estimated FC for the critical layers than the FC estimated using the generic correlation. This resulted in an increase in the normalized/corrected penetration resistance, shifting many of the plotted points to the right.
As may be observed from Figure 3, RW98, Mea06, and IB08 yield predictions that are mostly consistent with field observations for the case histories, but none of the procedures correctly predicted all cases. To quantitatively assess the relative predictive capabilities of the three alternative CPT-based liquefaction evaluation procedures, the error index (E_I) proposed by Green et al. (2014) is used:

$$E_I = \sum_{i=1}^{n} R_i \tag{1}$$

where n = number of case histories (i.e., 48),

$$R_i = \begin{cases} \left| \frac{CSR_{M7.5}}{K_\sigma} - CRR_{M7.5} \right| & \text{for "Liq" and "Minor Liq" cases where } \frac{CSR_{M7.5}}{K_\sigma} < CRR_{M7.5} \\ 0 & \text{for "Liq" and "Minor Liq" cases where } \frac{CSR_{M7.5}}{K_\sigma} \geq CRR_{M7.5} \end{cases}$$

$$R_i = \begin{cases} \left| \frac{CSR_{M7.5}}{K_\sigma} - CRR_{M7.5} \right| & \text{for "No Liq" cases where } \frac{CSR_{M7.5}}{K_\sigma} > CRR_{M7.5} \\ 0 & \text{for "No Liq" cases where } \frac{CSR_{M7.5}}{K_\sigma} \leq CRR_{M7.5} \end{cases}$$

The proposed error index will equal zero if all the predictions are consistent with field observations, but will increase in value as the number and "magnitude" of the mispredictions increases. On an individual case basis, R_i equals zero for a correct prediction of a "Liquefaction" or "No Liquefaction" case, but is equal to the vertical distance between the $CRR_{M7.5}$ curve and the plotted point for a mispredicted "Liquefaction" or "No Liquefaction" case.

The computed E_I values for each CPT-based liquefaction evaluation procedure are presented in Table 2. As may be observed, the IB08 gives predictions that are more consistent with field observations than the other procedures for the case histories analyzed in this paper. However, the computed E_I values for IB08 used in conjunction with the Robertson and Wride (1998) generic I_c-FC correlation are considerably lower (indicating predictions that are more consistent with field observations) than those when IB08 is used in conjunction with the Christchurch-specific correlation, which is opposite of what would be expected. RW98 yields the next most consistent predictions with field observations made during the Darfield earthquake, while the Mea06 with the V_{s12}-dependent r_d yielded more consistent predictions with field observations made during the Christchurch earthquake. The least consistent predictions with field observations made during both earthquakes result from the Mea06 procedure with the V_{s12}-independent r_d relation.

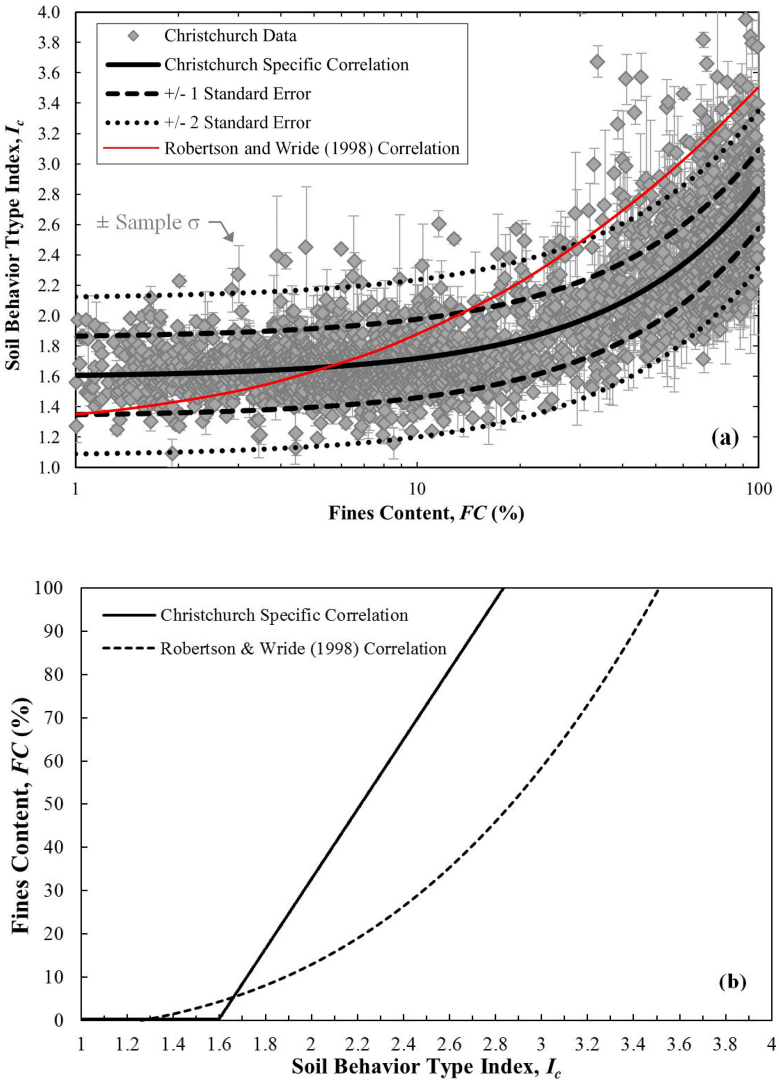

Figure 4. (a) Christchurch-specific I_c – FC data and proposed correlation; (b) Comparison of the Robertson and Wride (1998) generic Ic-FC correlation and Christchurch-specific correlation.

Table 2. Error Indices for the three CPT-based liquefaction evaluation procedures.

	E_I				
	RW98	Mea06 (V_{s12}-dep r_d)	Mea06 (V_{s12}-indep r_d)	IB08 (Generic I_c-FC correlation)	IB08 (Chch I_c-FC correlation)
Darfield eqk	0.264	0.379	0.411	0.113	0.223
Christchurch eqk	0.275	0.225	0.290	0.047	0.164
Total	0.539	0.604	0.701	0.167	0.387

Evaluation of CPT Liquefaction Evaluation Procedures Using the Liquefaction Potential Index

Overview of LPI

As mentioned in the Introduction, simplified liquefaction evaluation procedures only provide estimates of the FS against liquefaction triggering as a function of depth in a profile. They do not predict the severity of liquefaction manifestation at the ground surface, which more directly correlates to damage potential due to liquefaction. Various liquefaction damage index frameworks have been proposed to fill this gap, to include for example: LPI (Iwasaki et al., 1978); the Ishihara inspired LPI (LPI_{ISH}: Maurer et al., 2015c); and the Liquefaction Severity Number (LSN: van Ballegooy et al., 2014). The LPI framework is used herein to assess the predictive capabilities of the three alternative liquefaction evaluation procedures. LPI is computed as:

$$\mathrm{LPI} = \int_0^{20\ \mathrm{m}} \mathrm{F} \cdot \mathrm{w(z)}\ \mathrm{dz} \tag{2}$$

In this expression, F = 1 – FS for FS ≤ 1 and F = 0 for FS > 1, where FS is obtained from the simplified liquefaction evaluation procedure as described above, and w(z) is a depth weighting function given by w(z) = 10 – 0.5z, where z = depth in meters below the ground surface. Thus, it is assumed that the severity of liquefaction manifestation is proportional to the thickness of a liquefied layer; the amount by which FS is less than 1.0; and the proximity of the layer to the ground surface. It can be shown that the depth weighting function allots maximum contributions to LPI from the 1st, 2nd, 3rd, and 4th 5-meter depth increments of 43.75%, 31.25%, 18.75%, and 6.25%, respectively. Given this definition, LPI can range from 0 for a site with no liquefaction potential (i.e., FS ≥ 1 for all depths) to a maximum theoretical value of 100 for a site where FS is zero for all depths. Using SPT data from 45 liquefaction sites in Japan, Iwasaki et al. (1978) found that 80% of the sites had LPI > 5, while 50% had LPI > 15. Based on this data, it was proposed that severe liquefaction should be expected for sites where LPI >15 but should not be expected for sites where LPI < 5. This criterion for liquefaction manifestation, defined by two threshold values of LPI, is subsequently referred to herein as the *Iwasaki criterion*.

LPI has been widely adopted as a predictive proxy for liquefaction damage potential and has been used worldwide in hazard mapping, urban planning, and the engineering design of infrastructure (e.g., Sonmez, 2003; Biase et al., 2006; Holzer et al., 2006a; 2006b; Lenz and

Baise, 2007; Cramer et al., 2008; Hayati and Andrus, 2008; Holzer, 2008; Chung and Rogers, 2011; Kang et al., 2014). However, in using LPI to assess liquefaction hazard in current practice, it is not always appreciated that the efficacy of LPI hazard assessment (and the *Iwasaki criterion)* is inherently linked to the liquefaction evaluation procedure used within the LPI framework. Accordingly, the LPI framework can be used to assess the predictive capabilities of the RW98, Mea06, and IB08 liquefaction evaluation procedures. However, in contrast to using case histories for this purpose, as was done above, no additional judgement is needed within the LPI framework to select "critical layers" and their representative properties. This is significant because the interpretation of case histories is inherently subjective and, as a result, is often a point of contention among researchers. Also, interpretation of case histories is time consuming and circumventing this step (other than assessing the severity of the surficial liquefaction manifestations) allows a larger number of cases from the Canterbury earthquake sequence to be used to evaluate the predictive capabilities of the liquefaction evaluation procedures. However, as mentioned above, the use of the LPI has drawbacks and should be viewed as an alternative approach to assessing the predictive capabilities of the liquefaction evaluation procedures, rather than a superior approach. Specifically, the depth weighting factor used in LPI procedure may over-weight the influence of deeper layers and under-weight shallower layers on their contribution to the severity of surficial liquefaction manifestations (e.g., van Ballegooy et al., 2014a; Maurer et al., 2015c). Additionally, the LPI procedure does not appropriately account for the non-liquefiable crust and interbedded non-liquefiable layers suppressing the severity of surficial liquefaction manifestations (Maurer et al. 2015a,c).

Case Study Sites

Drawing from the over 20,000 CPT soundings performed in Christchurch and surrounding areas, 3,500 soundings at sites where the severity of liquefaction manifestation was well-documented following both the Darfield and Christchurch earthquakes were selected for use herein, resulting in 7,000 case studies. As detailed in Maurer et al. (2014a, 2015a, 2015b), in compiling the 3,500 soundings from the larger dataset, soundings were rejected from the study for one of several reasons, as explained in the following paragraphs.

First, CPT soundings were rejected if performed at sites where the predominant manifestation of liquefaction was lateral spreading. This distinction is made because lateral spreading is a unique manifestation of liquefaction, and because there are separate criteria for assessing its severity (e.g., Youd et al., 2002), including the ground slope and height of the nearest free-face (e.g., river bank). Consequently, while site profiles with thin liquefiable layers may have low LPI values, these sites are susceptible to lateral spreading if located on sloping ground or near rivers. Since the factors pertinent to lateral spreading cases are not considered in the formulation of LPI, such cases should not be used to assess the accuracy of LPI hazard assessment. *Second*, CPTs were rejected if the depth of "pre-drill" significantly exceeded the estimated depth of the ground water table (GWT), a condition arising at sites where buried utilities needed to be safely bypassed before testing could begin. While CPT data in the pre-drill zone may be estimated using intra-CPT extrapolation or inter-CPT interpolation, doing so below the GWT could lead to erroneous hazard assessments if the soil profile is misrepresented. *Third*, termination depths of

CPT soundings were geo-spatially analyzed using an Anselin Local Morans *I* analysis (Anselin, 1995) and soundings with anomalously shallow termination depths were rejected. As shown in Equation 2, LPI requires integration over 20 m depth. However, if the local subsurface geology is well-characterized, it may be known that dense, non-liquefiable soils are typically found at a particular depth and unlikely to be underlain by looser liquefiable deposits that contribute to LPI. Such is the case in Christchurch, where liquefiable deposits overlay the Riccarton Gravel formation. The Anselin (1995) analysis was thus used to identify soundings that may have terminated before reaching the Riccarton formation. For the remaining soundings, the termination depths were reasonably assumed to define the maximum depths of liquefiable strata.
As detailed in Maurer et al. (2014, 2015a, 2015b), the severity of surficial liquefaction manifestations following both the Darfield and Christchurch earthquakes was assessed for each of the CPT sounding locations. This was accomplished by using ground reconnaissance field notes and high-resolution aerial and satellite imagery (CGD, 2012) performed in the days immediately following each of the earthquakes. CPT sites were assigned one of four damage classifications described in Green et al. (2014): "no liquefaction," "minor liquefaction," "moderate liquefaction," and "severe liquefaction." Of the 7,000 case studies compiled, 49% are cases of "no manifestation," and 51% are cases where manifestation severity was classified as either "minor," "moderate," or "severe."

Given the sensitivity of liquefaction hazard and computed LPI values to GWT depth (e.g., Chung and Rogers, 2011; Maurer et al., 2014a), accurate measurement of GWT depth is critical. For this study, GWT depths were sourced from the robust, event-specific regional ground water models of van Ballegooy et al. (2014b). These models, which reflect seasonal and localized fluctuations across the region, were derived in part using monitoring data from a network of ~1000 piezometers and provide a best-estimate of GWT depths immediately prior to the Darfield and Christchurch earthquakes. Considering the extent and density of monitoring, the van Ballegooy et al. (2014b) GWT models in Christchurch are likely amongst the most robust ever used for regional study of liquefaction hazard assessment. Finally, soil unit weights were estimated for each procedure using the method of Robertson and Cabal (2010).

Evaluation of Existing Liquefaction Evaluation Procedures

Overview of Receiver-Operating-Characteristic (ROC) Analyses

To assess the predictive capabilities of the RW98, Mea06, and IB08 liquefaction evaluation procedures within the LPI framework, receiver-operating characteristic (ROC) analyses, or "ROC curves," are used. ROC curves have been widely adopted to analyze the performance of classifier systems, including extensive use in medical diagnostics (e.g., Zou, 2007), but by comparison, the use of ROC curves in geotechnical engineering is relatively limited (Chen et al., 2007; Oommen et al., 2010, Mens et al., 2012; Maurer et al., 2014b, 2015a,b). In any ROC curve application, the distributions of "positives" (e.g., liquefaction is observed) and "negatives" (e.g., no liquefaction is observed) overlap when the frequency of the distributions are expressed as a function of index test results (e.g., LPI values). In such cases, threshold values for the index test (e.g., *Iwasaki Criterion*) results are selected considering the relative probabilities of true

positives (i.e., liquefaction is observed, as predicted) and false positives (i.e., liquefaction is predicted, but is not observed). Setting the threshold too low will result in numerous false positives, which is not without consequences, while setting the threshold unduly high will result in many false negatives (i.e., liquefaction is observed when it is predicted not to occur), which comes with different consequences. ROC analyses are particularly valuable for evaluating the relative efficacy of alternative diagnostic tests, independent of the thresholds used, and for selecting an optimal threshold for a given diagnostic test.

In this study, the alternative diagnostic tests are the three alternative liquefaction evaluation procedures, and the index test results are the computed LPI values. Accordingly, in analyzing the case histories, true and false positives are scenarios where surficial liquefaction manifestations are predicted, and were and were not observed, respectively. Figure 5 illustrates the relationship among the positive and negative distributions, the selected threshold value, and the corresponding ROC curve, where the ROC curve plots the true and false positive probabilities for varying threshold values. In ROC curve space, random guessing is indicated by a 1:1 line through the origin (i.e., equivalent correct and incorrect predictions), while a perfect model plots as a point at (0,1), indicating the existence of a threshold value which perfectly segregates the dataset (e.g., all sites with manifestation have LPI above the selected threshold; all sites without manifestation have LPI below the same selected threshold). While no single parameter can fully characterize model performance, the area under a ROC curve (AUC) is commonly used for this purpose, where AUC is equivalent to the probability that sites with manifestation have higher computed LPI than sites without manifestation (e.g., Fawcett, 2005). As such, increasing AUC indicates better model performance. Also, use of AUC to assess predictive capabilities is ideal because it is independent of the severity threshold criteria used (e.g., *Iwasaki Criterion*), where the optimal threshold criterion has been shown to vary as a function of the liquefaction evaluation procedure used to evaluate a given site (Maurer et al., 2015b) and for a given liquefaction evaluation procedure, to vary as a function of the FC of the profile being analyzed (Maurer et al., 2015a). To place the computed AUC values in context for assessing the performance of the liquefaction evaluation procedures, AUCs of 0.5 and 1.0 indicate random guessing and perfect predictions, respectively.

Results and Discussion

Utilizing the 7,000 combined case studies from the Darfield and Christchurch earthquakes, LPI values were computed using the RW98, Mea06, and IB08 liquefaction evaluation procedures. For the Mea06 procedure, $CSR_{M7.5}$ values were only computed using the V_{S12}-independent r_d equation because shear wave profiles were not available for the majority of the 3,500 CPT sounding sites analyzed. For the IB08 procedure, both the Robertson and Wride (1998) generic I_c-FC correlation and the newly proposed Christchurch-specific correlation were used (Figure 4), designated below as IB08[1] and IB08[2], respectively. Additionally, for all the procedures, an I_c "cutoff" value of 2.6 was used (i.e., soils with $I_c \geq 2.6$ are assumed to be not susceptible to liquefaction) (Robertson and Wride, 1998).

The ROC curves are plotted in Figure 6 for all the liquefaction evaluation procedures for discerning sites with and without surficial liquefaction manifestations and the corresponding

AUC values are listed in Table 3. (Note that "True Positive Rate" and "False Positive Rate" used in Figure 6 are synonymous with "True Positive Probability" and "False Positive Probability," respectively, used in Figure 5.) As may be observed from Figure 6 and Table 3, all of the liquefaction evaluation procedures performed well for the sites analyzed. However, similar to findings above for the select case history analysis, IB08 yielded predictions that were more consistent with field observations than the other procedures, and Mea06 yielded predictions that were least consistent. In contrast to the findings from the analysis of select case histories, the predictive capabilities of IB08 within the LPI framework was independent of whether the generic I_c-FC correlation or the newly proposed Christchurch-specific correlation was used.

At first glance the findings from the use of select case histories and the LPI framework regarding the predictive capabilities of the IB08 used in conjunction with the two different I_c-FC correlations may seem at odds, but they actually are not. The reason for this is that AUC is being used to assess the predictive capabilities of the liquefaction evaluation procedures, as opposed to using a fixed threshold severity criterion. Equal AUC values for IB08[1] and IB08[2] implies that using the Christchurch-specific I_c-FC correlation versus the generic correlation results in a relatively constant shift in the computed FS for the cases with and without surficial liquefaction manifestations. This in turn results in a relatively constant shift in the computed LPI values for the two surficial manifestation severity datasets, rather than an increase or decrease in the overlap of the distributions of the computed LPI values for the two datasets (e.g., envision the two distributions shown in Figure 5a uniformly shifting either to the left or right). This constant shift in the computed LPI values inherently implies that the optimal severity threshold criterion for the Christchurch data will be dependent on which I_c-FC correlation is used in conjunction with IB08, which is consistent with the findings of Maurer et al. (2015a).

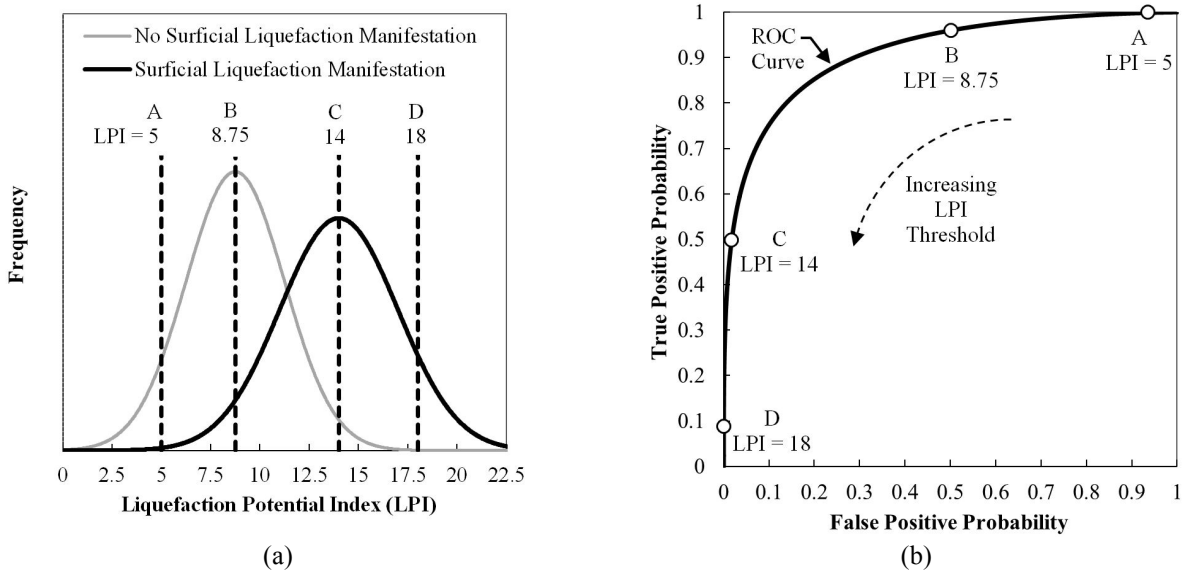

Figure 5. ROC analyses: (a) Frequency distributions of No Surficial Liquefaction Manifestation and Surficial Liquefaction Manifestation as a function of LPI, with four different threshold LPI values shown; and (b) Corresponding ROC curve.

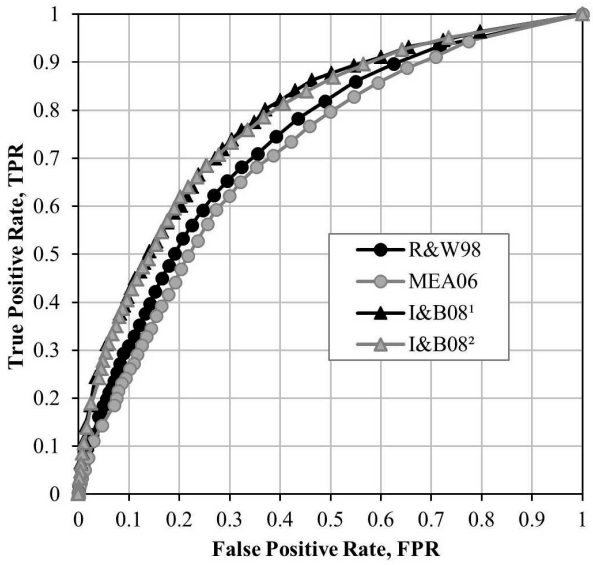

Figure 6. ROC analysis of liquefaction evaluation procedures used within the LPI framework for predicting the occurrence of surficial liquefaction manifestation.

Table 3. Computed AUC values for the liquefaction evaluation procedures.

	RW98	**Mea06**	**IB08[1]**	**IB08[2]**
AUC	0.74	0.71	0.78	0.78

Summary and Conclusions

The combination of well-documented liquefaction responses during multiple events, densely-recorded ground motions for the events, and detailed subsurface characterization in relation to the 2010-2011 Canterbury, New Zealand earthquake sequence provides an unprecedented opportunity to assess and advance the current state of practice for evaluating liquefaction triggering. Towards this end, this paper presents an updated analysis of 48 high-quality CPT liquefaction case histories originally presented in Green et al. (2014). The update includes the removal of one site from the original database due to concerns about the recorded sleeve friction values for CPT sounding from that site (reducing the database from 25 sites to 24 sites) and the use of a new Christchurch-specific correlation for estimating FC for use with IB08. The majority of the sites selected liquefied during the Darfield earthquake and either had no or only minor surficial liquefaction manifestations resulting from the Christchurch earthquake, or vice versa. Additionally, all sites were located relatively close to strong ground motion stations and were characterized by both CPT soundings and surface wave testing. The case histories were used to assess the predictive capabilities of three alternative, deterministic, CPT-based simplified liquefaction evaluation procedures that are in common use: RW98, Mea06, and IB08. Although all of the procedures yield predictions that are consistent with the field observations for the majority of the case histories, IB08 resulted in the lowest error index for the 48 case histories analyzed, with lower E_I values indicating more consistent predictions with field observations. However, E_I values for the IB08 when used in conjunction with the new Christchurch-specific I_c-

FC correlation were higher than when the generic correlation was used, and is similar to findings from an independent study by van Ballegooy (2015). This was not expected and implies that additional research is needed on treatment of FC effects in the IB08 procedure.

In addition to using a limited number of select case histories to assess the liquefaction evaluation procedures, the LPI framework was also used for this purpose. The advantage of using the LPI framework is that it circumvents the need to select the "critical layer" for each site, which inherently involves subjectivity, thus allowing a larger number of cases to be used in the assessment. The disadvantages of using the LPI procedure relates to the depth weighting factor inherent to the procedure and the lack of accounting for the influence of the non-liquefiable crust and interbedded non-liquefiable layers on the severity of surficial manifestations. Accordingly, use of the LPI procedure should be viewed as an alternative approach to assessing the predictive capabilities of the liquefaction evaluation procedures, and not necessarily a superior approach.

In total 3,500 CPT soundings were analyzed within the LPI framework for both the Darfield and Christchurch earthquakes, resulting in 7,000 case studies. The case study sites were selected to be regionally distributed across Christchurch and its environs and to have a relatively equal number of cases of observed and no observed post-earthquake surficial liquefaction manifestations. To quantify the predictive capabilities of the procedures the area under the ROC curves (AUC) was used, with possible values ranging from 0.5 (random guesses) to 1.0 (perfect predictions). As with the findings from the select case history analysis, all the procedures performed well, but IB08 yielded predictions that were the more consistent with field observations than the other procedures. However, AUC for the IB08 procedure were identical when both the generic and Christchurch-specific I_c-FC correlations were used. This implies that using the Christchurch-specific I_c-FC correlation versus the generic correlation results in a relatively constant shift in the computed FS for the cases with and without surficial liquefaction manifestations. This in turn results in a relatively constant shift in the computed LPI values for the two surficial manifestation severity datasets, rather than an increase or decrease in the overlap of the distributions of the computed LPI values for the two datasets. Additionally, the equal AUC values imply that the optimal LPI severity threshold criterion for the Christchurch data is dependent on the I_c-FC correlation used in conjunction with IB08.

Finally, it needs to be noted that the findings presented herein apply only to the ranges of the conditions evaluated. While the data from Darfield and Christchurch earthquakes add considerably to liquefaction knowledgebase, the ranges of the PGA, FC, M_w, and σ'_{vo} fall within the limits of the liquefaction databases used to develop RW98, Mea06, and IB08. Accordingly, the predictive capabilities of these procedures beyond these ranges cannot be assessed from the results presented herein.

Acknowledgments

This study is based on work supported by the U.S. National Science Foundation (NSF) grants CMMI-1030564, CMMI-1306261, and CMMI-1435494, and US Army Engineer Research and Development Center (ERDC) grant W912HZ-13-C-0035. The third and fourth authors would

like to acknowledge the continuous financial support provided by the Earthquake Commission (EQC) and Natural Hazards Research Platform (NHRP), New Zealand, of the research and investigations related to the 2010-2011 Canterbury earthquakes. The authors gratefully acknowledge the collaboration with L. Wotherspoon, B. Cox, C. Wood, S. van Ballegooy, J. Bray, T. O'Rourke, M. Taylor, K. Robinson, M. Pender, R. Orense, J. Zupan, among others, on various aspects of this research and the review comments from Drs. Sjoerd van Ballegooy, Ross Boulanger, Peter Robertson, and Jim Mitchell. The authors also acknowledge the New Zealand GeoNet project and its sponsors EQC, GNS Science, and LINZ for providing the earthquake occurrence data and the Canterbury Geotechnical Database and its sponsor EQC for providing the CPT soundings, lateral spread observations, and aerial imagery used in this study. However, any opinions, findings, and conclusions or recommendations expressed in this paper are those of the authors and do not necessarily reflect the views of NSF, ERDC, EQC, NHRP, or LINZ.

Notice

Some of the data used in this study was extracted from the Canterbury Geotechnical Database (https://canterburygeotechnicaldatabase.projectorbit.com), which was prepared and/or compiled for the Earthquake Commission (EQC) to assist in assessing insurance claims made under the Earthquake Commission Act 1993 and/or for the Canterbury Geotechnical Database on behalf of the Canterbury Earthquake Recovery Authority (CERA). The source maps and data were not intended for any other purpose. EQC, CERA, and their data suppliers and their engineers, Tonkin & Taylor, have no liability for any use of these maps and data or for the consequences of any person relying on them in any way.

References

Anselin L. Local Indicators of Spatial Association—LISA. *Geographical Analysis* 1995; **27**(2): 93–115.

ASTM D2487-11 *Standard Practice for Classification of Soils for Engineering Purposes (Unified Soil Classification System),* ASTM International, West Conshohocken, PA 2011.

Baise LG, Higgins RB, Brankman CM. Liquefaction hazard mapping-statistical and spatial characterization of susceptible units. *Journal of Geotechnical and Geoenvironmental Engineering* 2006; **132**(6): 705-715.

Bradley BA, Cubrinovski M. Near-source Strong Ground Motions Observed in the 22 February 2011 Christchurch Earthquake. *Seismological Research Letters* 2011; **82**: 853-865.

Bradley BA. Strong ground motion characteristics observed in the 4 September 2010 Darfield, New Zealand earthquake. *Soil Dynamics and Earthquake Engineering* 2012a; **42**: 32-46.

Bradley BA. Strong ground motion characteristics observed in the 4 September 2010 Darfield, New Zealand earthquake. *Soil Dynamics and Earthquake Engineering* 2012b; **42**: 32-46.

Bradley BA. Ground motions observed in the Darfield and Christchurch earthquakes and the importance of local site response effects. *New Zealand Journal of Geology and Geophysics* 2012c, **55**: 279-286.

Bradley BA. Site-specific and spatially distributed estimation of ground motion intensity in the 2010-2011 Canterbury earthquakes. *Soil Dynamics and Earthquake Engineering* 2014a; **61-62**: 83-91.

Bradley BA, Quigley M, Van Dissen R. Ground motion and seismic rupture aspects of the 2010-2011 Canterbury earthquake sequence, *Earthquake Spectra* 2014b; **30**(1): 1-15.

Brown LJ, Beetham RD, Paterson BR, Weebe, J.H. Geology of Christchurch, New Zealand. *Environmental and Engineering Geoscience* 1995; **1**: 427–488.

CGD - Canterbury Geotechnical Database. *Aerial Photography*, Map Layer CGD0010, See: https://canterburygeotechnicaldatabase. projectorbit.com. Accessed 1/12/12.

Cetin KO, *Reliability-based assessment of seismic soil liquefaction initiation hazard* 2000; Ph.D. dissertation, University of California, Berkeley, California.

Chen CC, Tseng CY, Dong JJ. New entropy-based method for variables selection and its application to the debris-flow hazard assessment. *Engineering Geology* 2007; **94**: 19-26.

Chung J, Rogers J. Simplified method for spatial evaluation of liquefaction potential in the St. Louis Area. *Journal of Geotechnical and Geoenvironmental Engineering* 2011; **137**(5): 505-515.

Cramer CH, Rix GJ, Tucker K. Probabilistic liquefaction hazard maps for Memphis, Tennessee. *Seismological Research Letters* 2008; **79**(3): 416-423.

Cousins J, McVerry G. Overview of strong motion data from the Darfield earthquake. *Bulletin of the NZSEE* 2010; **43**(4): 222-227.

Cubrinovski M, Green RA, eds. Geotechnical reconnaissance of the 2010 Darfield (Canterbury) earthquake, (contributing authors in alphabetical order: J. Allen, S. Ashford, E. Bowman, B. Bradley, B. Cox, M. Cubrinovski, R. Green, T. Hutchinson, E. Kavazanjian, R. Orense, M. Pender, M. Quigley, and L. Wotherspoon). *Bulletin of the New Zealand Society for Earthquake Engineering* 2010; **43**(4): 243-320.

Cubrinovski M, Bradley B, Wotherspoon L, Green RA, Bray J, Wood C, Pender M, Allen J, Bradshaw A, Rix G, Taylor M, Robinson K, Henderson D, Giorgini S, Ma K, Winkley A, Zupan J, O'Rourke T, DePascale G, Wells D, Geotechnical aspects of the 22 February 2011 Christchurch earthquake. *Bulletin of the New Zealand Society for Earthquake Engineering* 2011; **43**(4): 205-226.

Cubrinovski M, Robinson K, Taylor M, Hughes MM, Orense R. Lateral spreading and its impacts in urban areas in the 2010-2011 Christchurch earthquakes. *New Zealand Journal of Geology and Geophysics* 2012; **55**(3): 255-269.

Fawcett T. An introduction to ROC analysis. *Pattern Recognition Letters* 2005; **27**: 861-874.

Forsyth P, Barrell D, Jongens R. *Geology of the Christchurch area* 2008. Institute of Geological and Nuclear Sciences GNS Science 1:250,000 Geological Map 16, 67 p.

GeoNet. http://magma.geonet.org.nz/resources/quakesearch/ (last accessed 26 Nov 2012)

Goda K, Hong HP, Spatial correlation of peak ground motions and response spectra, *Bulletin of the Seismological Society of America* 2008; **98**(1): 354–465.

Green RA, Allen A, Wotherspoon L, Cubrinovski M, Bradley B, Bradshaw A, Cox B, Algie T. Performance of levees (stopbanks) during the 4 September M_w7.1 Darfield and 22 February 2011 M_w6.2 Christchurch, New Zealand, earthquakes. *Seismological Research Letters* 2011a; **82**(6): 939-949.

Green RA, Wood C, Cox B, Cubrinovski M, Wotherspoon L, Bradley B, Algie T, Allen J, Bradshaw A, Rix G. Use of DCP and SASW tests to evaluate liquefaction potential: Predictions vs. observations during the recent New Zealand earthquakes. *Seismological Research Letters* 2011b; **82**(6): 927-938.

Green RA, Cubrinovski M, Cox B, Wood C, Wotherspoon L, Bradley B, Maurer B. Select liquefaction case histories from the 2010-2011 Canterbury earthquake sequence. *Earthquake Spectra* 2014; **30**(1): 131-153.

Hayati H, Andrus RD. Liquefaction potential map of Charleston, South Carolina based on the 1986 earthquake. *Journal of Geotechnical and Geoenvironmental Engineering* 2008; **134**(6): 815-828.

Holzer TL, Bennett MJ, Noce TE, Padovani AC, Tinsley III, JC. Liquefaction hazard mapping with LPI in the greater Oakland, California, area. *Earthquake Spectra* 2006a; **22**(3): 693-708.

Holzer TL, Blair JL, Noce TE, Bennett MJ. Predicted liquefaction of east bay fills during a repeat of the 1906 San Francisco earthquake. *Earthquake Spectra* 2006b; 22(S2): S261-277.

Holzer TL. Probabilistic liquefaction hazard mapping. in Zeng, D., Manzari, M.T., & Hiltunen, D.R., *Geotechnical Earthquake Engineering and Soil Dynamics IV*: Sacramento, CA, ASCE Geotechnical Special Publication 181,

2008.

Idriss IM, Boulanger RW. *Soil liquefaction during earthquakes*. Monograph MNO-12, Earthquake Engineering Research Institute 2008, Oakland, CA, 261 pp.

Iwasaki T, Tatsuoka F, Tokida K, Yasuda S. A practical method for assessing soil liquefaction potential based on case studies at various sites in Japan. *Proceedings of the 2nd International Conference on Microzonation*, Nov 26-Dec 1, San Francisco, CA, USA, 1978.

Kang GC, Chung JW, Rogers RJ. Re-calibrating the thresholds for the classification of liquefaction potential index based on the 2004 Niigata-ken Chuetsu earthquake. *Engineering Geology* 2014; **169**: 30-40.

Lenz A, Baise LG. Spatial variability of liquefaction potential in regional mapping using CPT and SPT data. *Soil Dynamics and Earthquake Engineering* 2007; **27**: 690-702.

Maurer BW, Green RA, Cubrinovski M, Bradley BA. Evaluation of the Liquefaction Potential Index for assessing liquefaction hazard in Christchurch, New Zealand. *Journal of Geotechnical and Geoenvironmental Engineering* 2014a; **140**(7).

Maurer BW, Green RA, Cubrinovski M, Bradley BA. Assessment of aging correction factors for liquefaction resistance at sites of recurrent liquefaction: A study of the Canterbury (NZ) earthquake sequence. *Proc. 10th National Conference on Earthquake Engineering (10NCEE)*, Anchorage, AK, 21-25 July 2014b.

Maurer BW, Green RA, Cubrinovski M, Bradley BA. Fines-content effects on liquefaction hazard evaluation for infrastructure in Christchurch, New Zealand. *Soil Dynamics and Earthquake Engineering* 2015a; **76**: 58-68.

Maurer BW, Green RA, Cubrinovski M, Bradley BA. Assessment of CPT-based methods for liquefaction evaluation in a Liquefaction Potential Index (LPI) framework. *Geotechnique* 2015b; **65**(5): 328-336.

Maurer BW, Green RA, Taylor O-DS. Moving towards an improved index for assessing liquefaction hazard: Lessons from historical data. *Soils and Foundations* 2015c; **55**(4): 778-787.

Mens AMJ, Korff M, van Tol AF. Validating and improving models for vibratory installation of steel sheet piles with field observations. *Geotechnical and Geological Engineering* 2012; **30**(5): 1085-1095.

Moss RES, Seed RB, Kayen RE, Stewart JP, Der Kiureghian A, Cetin KO. CPT-based probabilistic and deterministic assessment of in situ seismic soil liquefaction potential. *Journal of Geotechnical and Geoenvironmental Engineering* 2006; **132**(8): 1032-1051.

Oommen T, Baise LG, Vogel R. Validation and application of empirical liquefaction models. *Journal of Geotechnical and Geoenvironmental Engineering* 2010; **136**: 1618-1633.

Orense RP, Kiyota T, Yamada S, Cubrinovski M, Hosono Y, Okamura M, Yasuda S. Comparison of liquefaction features observed during the 2010 and 2011 Canterbury earthquakes. *Seismological Research Letters* 2011; **82**(6): 905-918.

Quigley MC, Bastin S, Bradley BA. Recurrent liquefaction in Christchurch, New Zealand, during the Canterbury earthquake sequence. *Geology* 2013; **41** (4) p. 419-422.

Robertson PK, Cabal KL. Estimating soil unit weight from CPT, *2nd International Symposium on Cone Penetration Testing*, Huntington Beach, CA, USA, Paper #2-40. 2010.

Robertson PK, Wride CE. Evaluating cyclic liquefaction potential using the cone penetration test. *Canadian Geotechnical Journal* 1998; **35**(3): 442-459.

Robinson K, Cubrinovski M, Bradley BA. Comparison of actual and predicted measurements of liquefaction-induced lateral displacements from the 2010 Darfield and 2011 Christchurch Earthquakes. *Proc. 2013 Conference of the New Zealand Society for Earthquake Engineering (NZSEE 2013),* Wellington, New Zealand, 26-28 April 2013.

Sonmez H. Modification of the liquefaction potential index and liquefaction susceptibility mapping for a liquefaction-prone area (Inegol, Turkey). *Environmental Geology* 2003; **44**(7): 862-871.

van Ballegooy S. Personal communication with R. Green 2015.

van Ballegooy S, Malan P, Lacrosse V, Jacka ME, Cubrinovski M, Bray JD, O'Rourke TD, Crawford SA, Cowan H. Assessment of liquefaction-induced land damage for residential Christchurch. *Earthquake Spectra* 2014a; **30**(1): 31-55.

van Ballegooy S, Cox SC, Thurlow C, Rutter HK, Reynolds T, Harrington G, Fraser J, Smith T. *Median water table elevation in Christchurch and surrounding area after the 4 September 2010 Darfield earthquake: Version 2*. GNS Science Report 2014/18, 2014b.

Wotherspoon LM, Pender MJ, Orense RP. Relationship between observed liquefaction at Kaiapoi following the 2010 Darfield earthquake and former channels of the Waimakariri River. *Engineering Geology 2012*; **125**: 45-55.

Youd TL, Hansen CM, Bartlett SF. Revised multilinear regression equations for prediction of lateral spread displacement. *Journal of Geotechnical and Geoenvironmental Engineering* 2002; **128**(12): 1007-1017.

Zou KH. *Receiver operating characteristic (ROC) literature research*. On-line bibliography available from: <http://www.spl.harvard.edu/archive/spl-pre2007/pages/ppl/zou/roc.html> accessed 15 March 2014. 2007.